THE JOURNAL OF BIOLOGICAL CHEMISTRY VOL. 284, NO. 44, pp. 30508–30517, October 30, 2009

Conformational Changes in Bcl-2 Pro-survival Proteins Determine Their Capacity to Bind Ligands*[S]

Received for publication, July 2, 2009, and in revised form, August 20, 2009 Published, JBC Papers in Press, September 2, 2009, DOI 10.1074/jbc.M109.040725

Erinna F. Lee, Peter E. Czabotar, Hong Yang, Brad E. Sleebs, Guillaume Lessene, Peter M. Colman, Brian J. Smith[1], and W. Douglas Fairlie[2]

From The Walter and Eliza Hall Institute of Medical Research, 1G Royal Parade, Parkville, Victoria 3052, Australia

Antagonists of anti-apoptotic Bcl-2 family members hold promise as cancer therapeutics. Apoptosis is triggered when a peptide containing a BH3 motif or a small molecule BH3 peptidomimetic, such as ABT 737, binds to the relevant Bcl-2 family members. ABT-737 is an antagonist of Bcl-2, Bcl-x_L, and Bcl-w but not of Mcl-1. Here we describe new structures of mutant BH3 peptides bound to Bcl-x_L and Mcl-1. These structures suggested a rationale for the failure of ABT-737 to bind Mcl-1, but a designed variant of ABT-737 failed to acquire binding affinity for Mcl-1. Rather, it was selective for Bcl-x_L, a result attributable in part to significant backbone refolding and movements of helical segments in its ligand binding site. To date there are few reported crystal structures of organic ligands in complex with their pro-survival protein targets. Our structure of this new organic ligand provided insights into the structural transitions that occur within the BH3 binding groove, highlighting significant differences in the structural properties of members of the Bcl-2 pro-survival protein family. Such differences are likely to influence and be important in the quest for compounds capable of selectively antagonizing the different family members.

Apoptosis, or programmed cell death, is a fundamental cellular process required by all multicellular organisms for the elimination of redundant, damaged, or potentially dangerous cells (1). A consequence of dysregulated cell death is the survival of abnormal cells, which in some cases can proliferate uncontrollably and form tumors. Hence, strategies to activate cell death pathways may represent one avenue by which cancer cells can be killed. A major pathway to cell death is regulated by the Bcl-2 family of proteins that consists of both pro-apoptotic and pro-survival members (2). Those family members that promote cell death are divided into two subgroups; that is, the Bax/Bak molecules, which are the essential mediators of apoptosis, and the BH3-only proteins (such as Bim, Bad, Puma, Noxa, and several others), which are the initiators of the apoptotic cascade. Within the pro-survival faction there are five members including Bcl-2 itself, Bcl-x_L, Bcl-w, Mcl-1, and A1. Overexpression of pro-survival proteins can confer a survival advantage to cancer cells. Critically, conventional anti-cancer therapies are often rendered ineffective by this overexpression and other up-stream defects, most prominently mutations in the tumor suppressor p53.

One strategy to kill cancer cells is to develop molecules that can mimic the BH3-only proteins (3). These proteins function by engaging the pro-survival proteins, although the downstream consequences of this interaction remain controversial (4). These interactions are mediated by a short sequence motif called the BH3 domain on the BH3-only protein. The structures of a number of BH3 domains in complex with pro-survival proteins have been solved, and all reveal that the BH3 sequence forms an amphipathic helix that inserts into a hydrophobic groove on the surface of the pro-survival proteins (5–10). These structures suggest that it might be possible to develop drugs based on small organic molecules that mimic natural BH3 ligands and activate the cell death pathways.

Although a number of "BH3-mimetic" molecules have now been described (11–21), many of these appear to kill cells in a non-mechanism-based manner (22). Only ABT-737, developed by Abbott Laboratories (15, 23), has been shown to be a *bona fide* BH3-mimetic (22, 24), binding in the same hydrophobic groove of Bcl-x_L as do BH3 ligands (25). ABT-263, a molecule in the same chemical class as ABT-737, has shown efficacy as a single agent in cancer cell lines and animal models of cancer (26–28) and is currently in a phase I/II clinical trial in leukemia and lymphoma patients.

One of the important aspects of BH3 peptide interactions with pro-survival proteins is selectivity; some BH3 ligands only bind certain subsets of pro-survival proteins (*e.g.* Bad only binds Bcl-x_L, Bcl-2, and Bcl-w, whereas Noxa only binds Mcl-1 and A1), but others such as Bim and Puma are more promiscuous and bind all pro-survival proteins tightly (29–31). This selectivity has important implications as it appears that a range of pro-survival proteins needs to be neutralized for cell death to proceed in some cell types (30, 32–34). Selectivity is also an important issue for drug potency. ABT-737 and ABT-263 share

* This work was supported by Australian National Health and Medical Research Council Program fellowships (to W. D. F. and P. M. C.) and Grant 461221 (to P. M. C.) and Project Grant 575561 (to P. E. C.), Leukemia and Lymphoma Society Grant SCOR 7015-02, Cancer Council of Victoria Grant-in-aid 461239 (to W. D. F.) and a fellowship (to E. F. L.), Leukemia Foundation of Australia Phillip Desbrow post doctoral fellowship (to E. F. L.), and by the Australian Cancer Research Foundation (to P. M. C.).

[S] The on-line version of this article (available at http://www.jbc.org) contains supplemental Figs. 1 and 2.

The atomic coordinates and structure factors (codes 3INQ, 3IO9, and 3IO8) have been deposited in the Protein Data Bank, Research Collaboratory for Structural Bioinformatics, Rutgers University, New Brunswick, NJ (http://www.rcsb.org/).

[1] To whom correspondence may be addressed: Structural Biology Division, The Walter and Eliza Hall Institute, 1G Royal Pde, Parkville, Victoria 3052, Australia. Tel.: 61-3-9345-2555; Fax: 61-3-9345-2686; E-mail: bsmith@wehi.edu.au.

[2] To whom correspondence may be addressed: Structural Biology Division, The Walter and Eliza Hall Institute, 1G Royal Pde, Parkville, Victoria 3052, Australia. Tel.: 61-3-9345-2555; Fax: 61-3-9345-2686; E-mail: fairlie@wehi.edu.au.

the same binding profile as Bad, and consequently, their efficacy seems to be restricted to cells/tumors in which Mcl-1 (to which they do not bind with high affinity) is inactivated or limiting (22, 28, 35–38). Hence, only a small subset of all tumors, in particular some hematological malignancies and small-cell lung cancers, appear to respond to ABT-737/ABT-263 when used as a single agent (15, 28). Therefore, to expand the repertoire of cancers that could be treated with BH3 mimetics, it is likely that the range of binding specificities of such molecules also needs to be expanded, with Mcl-1 being an obvious target candidate. Obatoclax (GX15-070), a small molecule developed by Gemin X Biotechnologies, has been reported to function in this way (14). However, this compound can kill cells deficient in both Bax and Bak, the essential mediators of apoptotic cell death (28); hence, its true mechanism of action is uncertain.

Peptide ligands can provide a template for small molecule drug design, particularly when a structure is available for it in complex with its target. For example, highly effective small molecule antagonists of the inhibitors of apoptosis proteins were designed using peptides as a starting point (39, 40). Antagonists of Bcl-x_L based on derivatized terphenyl and terephthalamide scaffolds that apparently mimic the BH3 α-helix have also been reported (17, 18), although in this case no complexes with the protein target have yet been described.

Here we use mutagenesis data and structures of BH3 peptides in complex with pro-survival proteins to guide attempts to develop a BH3-mimetic that binds to Mcl-1. Although that goal was not achieved, our results demonstrate extreme conformational flexibility in the pro-survival protein Bcl-x_L and yielded a novel Bcl-x_L-selective antagonist. In contrast, Mcl-1 displays no backbone conformational flexibility when presented with the various ligands we describe.

EXPERIMENTAL PROCEDURES

Compounds—ABT-737 was supplied by Abbott Laboratories. The synthesis of W1191542 is described in the supplemental material.

Protein Expression and Purification/Peptides—Expression and purification of the loop-deleted form of human Bcl-x_L (Δ27–82 ΔC24) and the human/mouse chimeric Mcl-1 (ΔN170 ΔC23) used for crystallization was performed as described previously (5, 41). Biacore assays were performed using human Bcl-2 ΔC22, Bcl-x_L ΔC24, Bcl-w C29S/A128E ΔC29, and human/mouse Mcl-1 ΔN170 ΔC23 purified as described previously (5, 35). Human Bim BH3 peptides (26-mers) were synthesized and purified by reverse phase high performance liquid chromatography to >90% purity by Mimotopes. All peptides used for crystallization have a free amine at the N terminus and are either amidated (wild-type Bim and L12F) or have a free acid (L12Y) at the C terminus. The wild-type Bim BH3 sequence used here is ^{1}DMRPEIWIAQELRRIGDEFNAYYARR^{26}.

Crystallization—Crystals of Bcl-x_L and Mcl-1 complexes with Bim BH3 peptides and with compounds were obtained by mixing the protein and ligand at a molar ratio of 1:1.3, then concentrating the sample to 10 mg/ml. Crystals were grown by the sitting drop method at room temperature under the following conditions: BimL12Y·Mcl-1 (0.15 M zinc acetate, 0.15 M imidazole, pH 5.75), W1191542·Bcl-x_L (0.2 M calcium acetate, 10% (w/v) polyethylene glycol 8000, 0.1 M imidazole, pH 8.0), Bim·Bcl-x_L (1 M sodium citrate, 0.1 M sodium cacodylate, pH 6.5), BimL12F·Bcl-x_L (0.02 M zinc acetate, 2.5 M NaCl, 0.1 M imidazole, pH 8.0). Prior to flash-freezing in liquid N_2, crystals were equilibrated into cryoprotectant consisting of reservoir solution plus increasing concentrations of ethylene glycol to a final concentration of 20% (v/v) for all complexes except BimL12Y·Mcl-1 where the final concentration was 25% (v/v).

Crystal Data Collection and Structure Refinement—X-ray data were collected at 100 K using an in-house RAXIS-IV++ detector with a micro-max007 rotating anode x-ray source or at the Australian synchrotron (42). All data were integrated and scaled with HKL2000 (43) (Table 1). Most structures were determined by molecular replacement with PHASER (44–46) using the following coordinates as search models: W1191542·Bcl-x_L (PDB 3FDL (47)), Bim·Bcl-x_L (PDB 2P1L (48)), BimL12F·Bcl-x_L (PDB 2P1L). In each case the ligand and solvent was removed before calculation. For BimL12Y·Mcl-1 a rigid body refinement in Refmac5 was performed using the structure of Mcl-1 in which the Leu-12 residue was mutated to alanine (PDB 2NL9 (5)). Several rounds of building in COOT (49) and refinement in REFMAC5 (50) and PHENIX (51) led to the final models. The crystals of BimL12F·Bcl-x_L were twinned, exhibiting a twinning fraction of 0.407, determined, and refined in PHENIX.

Cytochrome c Release Assay—The ability of peptides or compounds to elicit cytochrome *c* release from digitonin-permeabilized cells was examined as described previously (37). Mitochondria-containing crude lysates from *mcl-1*$^{-/-}$ or *bcl-x*$^{-/-}$ mouse embryonic fibroblasts (MEFs)[3] were incubated with 10 μM peptide or compound for 1 h at 30 °C before pelleting intact mitochondria. The supernatant was retained as the soluble fraction. The pellet fraction containing intact mitochondria was then lysed with buffer containing 1% (v/v) Triton X-100. The amount of cytochrome *c* in the soluble and pellet fractions was determined by Western blot using an anti-cytochrome *c* antibody (7H8 C12; BD Biosciences).

Cell Killing Assays—Short-term cell viability assays were measured using the CellTitre-Glo Luminescent Cell Viability Assay (Promega). Mouse embryonic fibroblasts (*mcl-1*$^{-/-}$ and *bcl-x*$^{-/-}$) were plated at 3000 cells/well in a 96-well plate overnight. The media was then replaced with fresh media containing serial dilutions of W1191542, ABT-737, or solvent (DMSO), and the cells incubated for a further 24 h. CellTitre-Glo reagent was then added, and the luminescent signal was determined with a luminometer. Percentage viability was determined as the ratio of the signal in the presence of compound to the signal obtained for wells in which only DMSO was added.

For long term clonogenic survival assays, *mcl-1*$^{-/-}$ and *bcl-x*$^{-/-}$ MEFs were plated at 150 cells/well in 6-well plates then incubated for 6 days in the presence of serial dilutions of ABT-737, W1191542, or solvent (DMSO). Colonies were then stained with Coomassie Blue and scored. Results were expressed as the ratio of the number of colonies in the presence of compound to the number of colonies in the presence of DMSO only.

[3] The abbreviation used is: MEF, mouse embryonic fibroblast.

TABLE 1

Crystallographic statistics for Mcl-1 and Bcl-x_L protein complexes

Numbers in parenthesis are for the highest resolution shell.

Data Set	BimL12Y·Mcl-1	W1191542·Bcl-x_L	Bim·Bcl-x_L	BimL12F·Bcl-x_L
PDB	3IO9	3INQ	3FDL	3IO8
Crystal parameter, space group	I222	$P2_12_12_1$	C2	$P6_2$
Unit cell parameters	a = 52.5 Å b = 74.1 Å c = 117.5 Å	a = 62.6 Å b = 68.2 Å c = 71.4 Å	a = 74.11 Å b = 35.68 Å c = 62.76 Å β = 111.5 °	a = 65.7 Å c = 170.1 Å
Data collection				
Wavelength (Å)	1.5418	1.5418	1.5418	0.9566
Resolution (Å)	50.00-2.20 (2.28-2.20)	50.00-2.00 (2.07-2.00)	50.00-1.78 (1.84-1.78)	50.00-2.30 (2.38-2.30)
R_{merge}	0.086 (0.378)	0.086 (0.867)	0.046 (0.163)	0.147 (0.835)
$I/\sigma(I)$	25.7 (6.0)	31.4 (2.3)	33.7 (11.1)	15.7 (2.7)
Completeness (%)	98.0 (99.1)	99.9 (99.9)	96.0 (94.9)	99.8 (99.3)
Redundancy	6.5 (5.4)	6.8 (6.3)	5.7 (5.8)	7.4 (5.8)
No. of copies/asymmetric unit	1	2	1	2
Temperature	100 K	100 K	100 K	100 K
Refinement				
Resolution (Å)	29.39-2.40 (2.46-2.40)	31.63-2.00 (2.09-2.00)	29.19-1.78 (1.82-1.78)	47.30-2.30 (2.39-2.30)
No. of reflections R_{work}	8,615 (610)	21,183 (2450)	13,529 (946)	18,425 (1,925)
No. of reflections R_{free}	474 (40)	1,090 (126)	728 (50)	948 (111)
R_{work}	0.209 (0.175)	0.194 (0.285)	0.160 (0.239)	0.185 (0.317)
R_{free}	0.251 (0.242)	0.250 (0.364)	0.208 (0.300)	0.231 (0.319)
No. of atoms				
Protein	1,146	2,272	1,163	2,319
Ligand	207	110	222	368
Solvent	70	182	209	32
Root mean square deviations				
Bond lengths (Å)	0.013	0.013	0.015	0.004
Bond angles (°)	1.4	1.4	1.5	0.76
Chiral ($Å^3$)	0.096	0.095	0.265	0.055

Binding Assays—Binding of compounds to pro-survival proteins was measured by surface plasmon resonance using a Biacore 3000 biosensor for solution competition assays as described previously (30). In these assays proteins were added at a final concentration of 10 nM and the compounds were diluted from 10 mM stock prepared in dimethyl sulfoxide. The running/dilution buffer was 10 mM Hepes, 150 mM NaCl, 3.4 mM EDTA, 0.005% (v/v) Tween 20, pH 7.2. Direct binding assays were performed using a Biacore S51 biosensor as previously described (52). The running buffer was 10 mM NaH_2PO_4, 40 mM Na_2HPO_4, 150 mM NaCl, 1.0 mM EDTA, 0.03% (v/v) Tween 20, 5% (v/v) DMSO, pH 7.4. Dilutions of each compound were injected at a flow rate of 90 μl/min over three spots (spot 1, immobilized with anti-GST antibody only; spot 2, coated with GST-Bcl-x_L captured by the anti-GST antibody; spot r, free) at 25 °C. The association time and dissociation times were 90 and 240 s, respectively. Buffer blanks without or containing 4–6% (v/v) DMSO were injected periodically for double referencing and solvent correction. All sensorgrams were processed using double referencing; first, the response from the reference spot (spot 1) was subtracted from the binding response (spot 2) followed by solvent correction, then the response from an average of the buffer injections was subtracted. To obtain kinetic rate constants (k_a and k_d), corrected response data were then fitted to a one-to-one binding site model that included mass transport limitations. The equilibrium dissociation constant (K_D) was determined from the ratio k_d/k_a.

RESULTS

Structure of BimL12Y·Mcl-1—BH3 domain peptides present four conserved hydrophobic residues (h1–h4) on one face of an amphipathic helix that bind into four pockets within the hydrophobic ligand binding groove on the pro-survival protein (5, 7, 10). In the 26-mer Bim BH3 peptides used here (^{1}DMRPEIW**I**AQE**L**RR**I**GDE**F**NAYYARR^{26}), these four hydrophobic amino acids are Ile-8, Leu-12, Ile-15, and Phe-19 (shown in bold). The structure of Bcl-x_L in complex with ABT-737 demonstrates that the chlorobiphenyl and thiophenyl groups of ABT-737 occupy pockets accommodating Leu-12 and Phe-19 in the Bim BH3 complex (25). In associated saturation mutagenesis studies we also showed that Mcl-1 is highly tolerant of any side-chain substitutions at the h4 residue of Bim (25), consistent with the structure of the Bim·Mcl-1 complex which shows that the h4 binding site on Mcl-1 is poorly formed and exposed to solvent compared with the corresponding region on Bcl-x_L (5, 7). We, therefore, decided to focus on the h2 binding pocket on Mcl-1 as a potential site that restricts ABT-737 from binding to it tightly.

Our mutagenesis studies also showed that although substitution of the h2 leucine residue on Bim for tyrosine caused a significant reduction in binding affinity for Mcl-1 compared with all other pro-survival proteins where only a minor effect on binding was observed (*i.e.* 60-fold decrease in affinity for Mcl-1 compared with wild-type Bim *versus* a 3-fold decrease for Bcl-x_L) (25), this mutant still bound Mcl-1 with ~470 nM affinity. As a tyrosine side chain bears some resemblance to the terminal chlorophenyl group of ABT-737, we reasoned that a structure of the Bim BH3 domain with the L12Y mutation in complex with Mcl-1 could provide some insights into how ABT-737 could be modified to bind Mcl-1.

We determined the x-ray structure at 2.2 Å resolution of human/mouse chimeric Mcl-1 (5) with a 26-residue Bim BH3

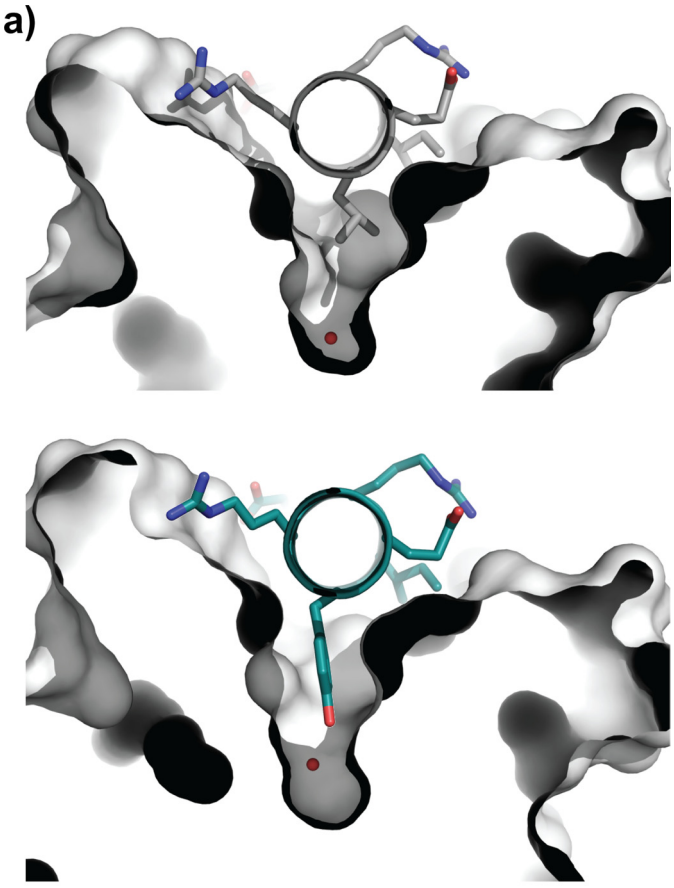

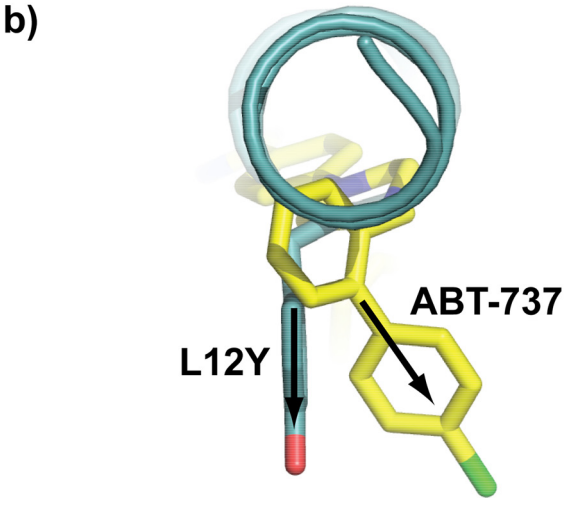

FIGURE 1. **Structure of BimL12Y·Mcl-1 complex.** *a*, comparison of Leu-12 and L12Y binding pockets on wild-type (PDB 2NL9) and mutant Bim BH3 peptides bound to Mcl-1. The tyrosine at position 12 in the Bim mutant peptide (*lower panel*) penetrates the h2 binding pocket deeper than the wild-type leucine residue. A water molecule (indicated in *red*) is seen at the bottom of the pocket in both structures. *b*, overlay of Mcl-1 and Bcl-x_L structures in their respective complexes with BimL12Y (*teal*) and ABT-737 (*yellow*, PDB 2YXJ), showing only the peptide and organic ligand. The tyrosine in BimL12Y penetrates the h2 pocket to approximately the same depth that the chlorobiphenyl group of ABT-737 penetrates the corresponding pocket of Bcl-x_L; however, the angle of entry (*arrows*) is different.

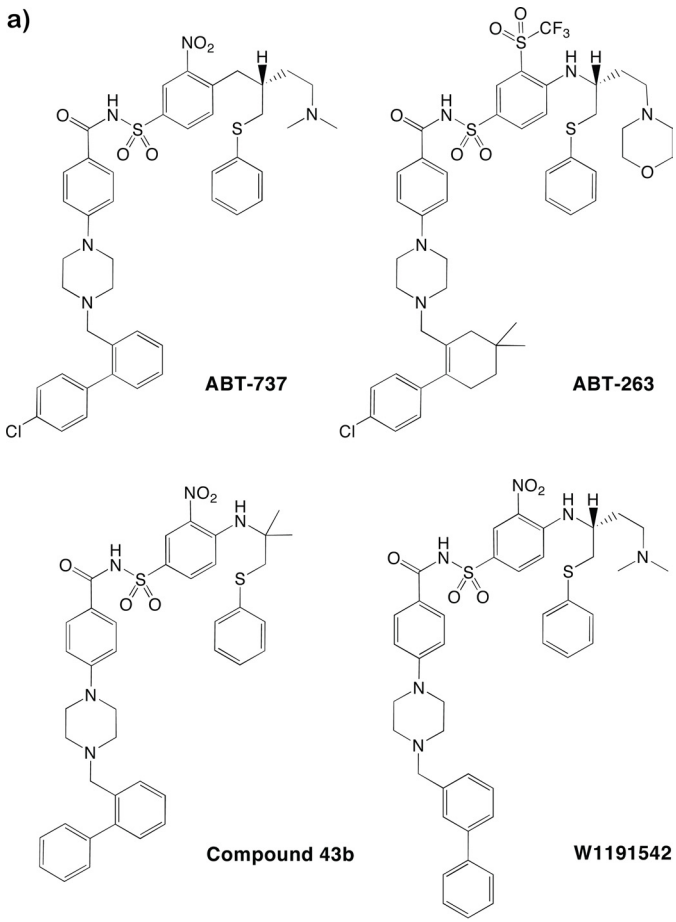

b)

	ABT-737	W1191542
Bcl-x_L	6	11
Bcl-w	25	230
Bcl-2	6	130
Mcl-1	>> 10,000	>> 10,000

FIGURE 2. **A designed ABT-737 derivative, W1191542.** *a*, chemical structures of ABT-737, ABT-263, Compound 43b (23) and W1191542. *b*, the IC_{50} values (in nM) determined by solution competition assays for either ABT-737 or W1191542 binding mammalian pro-survival proteins. ABT-737 binds tightly to Bcl-x_L, Bcl-w, and Bcl-2, whereas W1191542 demonstrates a more selective binding profile for Bcl-x_L.

peptide in which the h2 leucine residue was replaced with tyrosine (L12Y, see Table 1 for crystallographic statistics). The crystals grow under identical conditions and with similar cell dimensions to those of the wild-type peptide complex (5). The structure shows no significant differences in chain tracing between wild-type and mutant complexes. Only minor structural changes within the h2 binding pocket are observed, allowing the protein to accommodate the bulkier tyrosine residue which projects more deeply into this pocket than does the wild-type leucine residue at this position (Fig. 1*a*). This deep penetration of the h2 pocket is somewhat reminiscent of the way in which the chlorobiphenyl group on ABT-737 associates with the Bcl-x_L h2 pocket. Notably though, the angle at which the tyrosine residue enters the Mcl-1 h2 pocket compared with the way in which the chlorobiphenyl of ABT-737 enters the corresponding region on Bcl-x_L is different (Fig. 1*b*). Hence, although Mcl-1 can accommodate a bulky aromatic group on a peptidic ligand in the h2 binding pocket, it appears to do so differently to Bcl-x_L, at least in the context of a small molecule ligand.

Modifying ABT-737 to Mimic BimL12Y—The BimL12Y·Mcl-1 structure suggested a strategy by which ABT-737 could

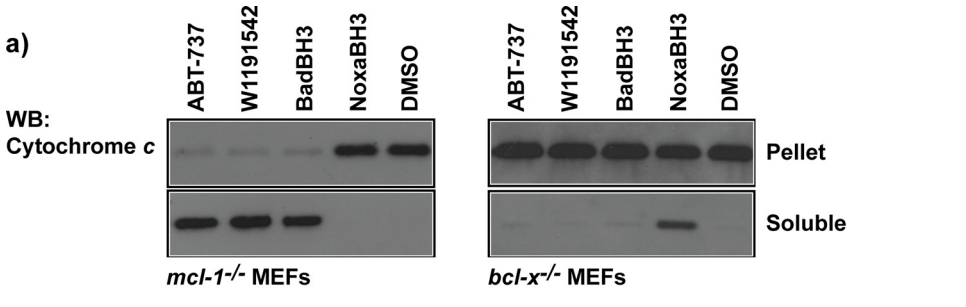

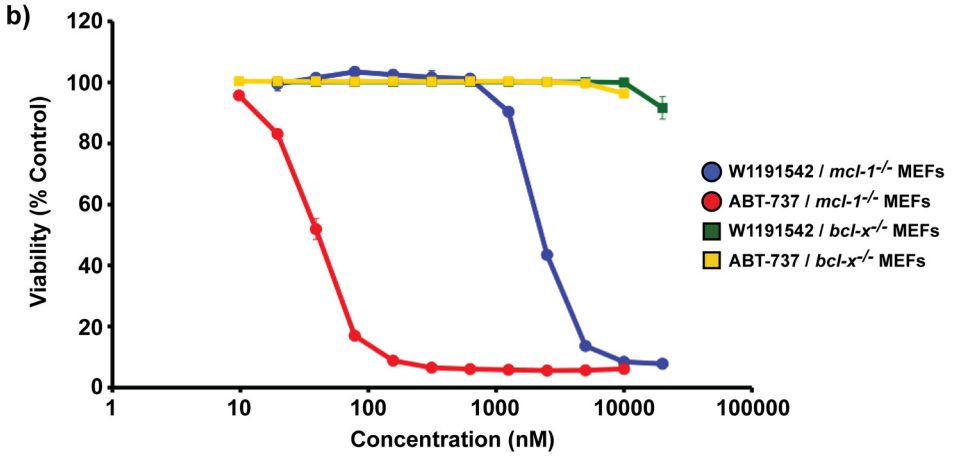

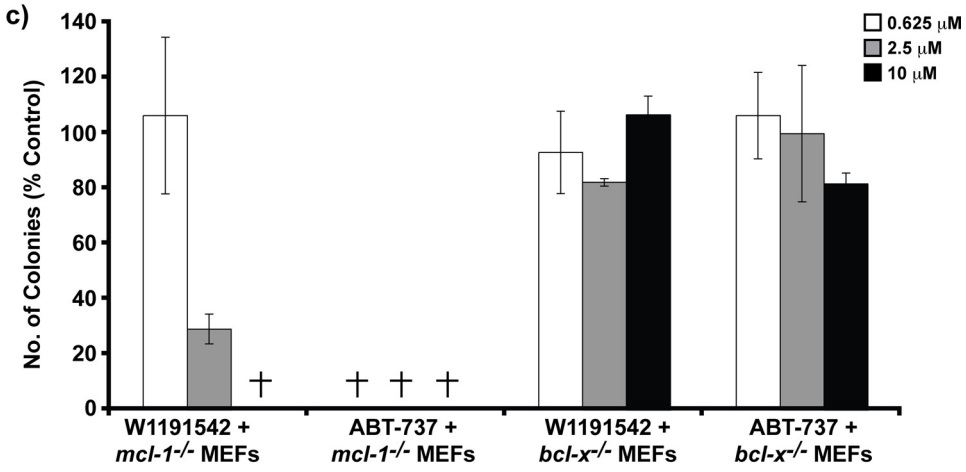

d)

	k_a (1/Ms)	k_d (1/s)	K_D (nM)
ABT-737	1.1×10^{6}	6.8×10^{-4}	0.6
W1191542	3.1×10^{6}	3.6×10^{-3}	1.2

FIGURE 3. **Biological functioning of W1191542.** *a*, W1191542 elicits cytochrome *c* release from digitonin-permeabilized *mcl-1*$^{-/-}$ MEFs, similar to ABT-737 and Bad BH3 domain peptide but not *bcl-x*$^{-/-}$ MEFs, evidenced by its translocation into the soluble fraction. *WB*, Western blot. *b* and *c*, W1191542 kills MEFs deficient in Mcl-1 in short-term (24 h) (*b*) viability and long term (6 days) clonogenic assays (*c*) but is significantly less efficacious than ABT-737. *Crosses* indicate the absence of colony formation. *d*, binding kinetics of ABT-737 and W1191542 to Bcl-x_L. W1191542 binds Bcl-x_L more rapidly but dissociates faster than ABT-737.

be modified to gain binding to Mcl-1. Switching the chlorophenyl group from the *ortho* to *meta* position more closely recapitulates the bond entry vector observed for the tyrosine residue in the Bim L12Y peptide complex with Mcl-1, potentially allowing it to engage the h2 binding pocket. We synthesized the compound (W1191542), although with a phenyl group in place of the chlorophenyl (Fig. 2*a*), as our mutagenesis studies showed that a phenylalanine substitution at Leu-12 in Bim BH3 was better tolerated in Mcl-1 (binding with 10 nM affinity) than the tyrosine substitution (25).

To determine whether W1191542 had gained binding affinity for Mcl-1, we performed solution competition assays using a Biacore biosensor (Fig. 2*b*). No apparent increase in affinity for Mcl-1 was observed. However, this compound retained high affinity binding to Bcl-x_L and indeed became significantly more selective for Bcl-x_L over Bcl-2 and Bcl-w compared with ABT-737. Hence, a subtle alteration in the structure of ABT-737 significantly influenced its binding selectivity profile, although not in the way intended.

W1191542 Retains Biological Activity—Although our initial aim in modifying ABT-737 to bind Mcl-1 was not achieved, W1191542 was still of interest because of its selective binding profile for Bcl-x_L. To test whether it retained biological activity, it was initially examined in an *in vitro* cytochrome *c* release assay using digitonin-permeabilized MEFs. As neutralization of both Mcl-1 and Bcl-x_L is required for cell killing in MEFs (33), we initially used cells deficient in Mcl-1 (*mcl-1*$^{-/-}$ MEFs) to remove the Mcl-1 "brake" on Bak/Bax. In this assay W1191542 was able to cause cytochrome *c* release similar to both ABT-737 and the Bad BH3 domain peptide (Fig. 3*a*), both of which target a wider subset of pro-survival proteins (Bcl-x_L, Bcl-2 and Bcl-w) with high affinity (15, 30). As a control, Bcl-x_L-deficient MEFs were also examined, and no cytochrome *c* release was observed with W1191542, although release was observed with the Noxa BH3 domain peptide that specifically targets Mcl-1 (30) (Fig. 3*a*).

To test whether W1191542 could induce apoptosis in intact cells, we examined its ability to kill *mcl-1*$^{-/-}$ MEFs. Although significant activity in a 24-h assay was observed (EC_{50}, 2 μM), it was several orders of magnitude weaker than ABT-737 (Fig. 3*b*). No killing of *bcl-x*$^{-/-}$ cells was observed (Fig. 3*b*), consistent with the binding data showing there was no significant affinity of this compound for Mcl-1. W1191542 was also exam-

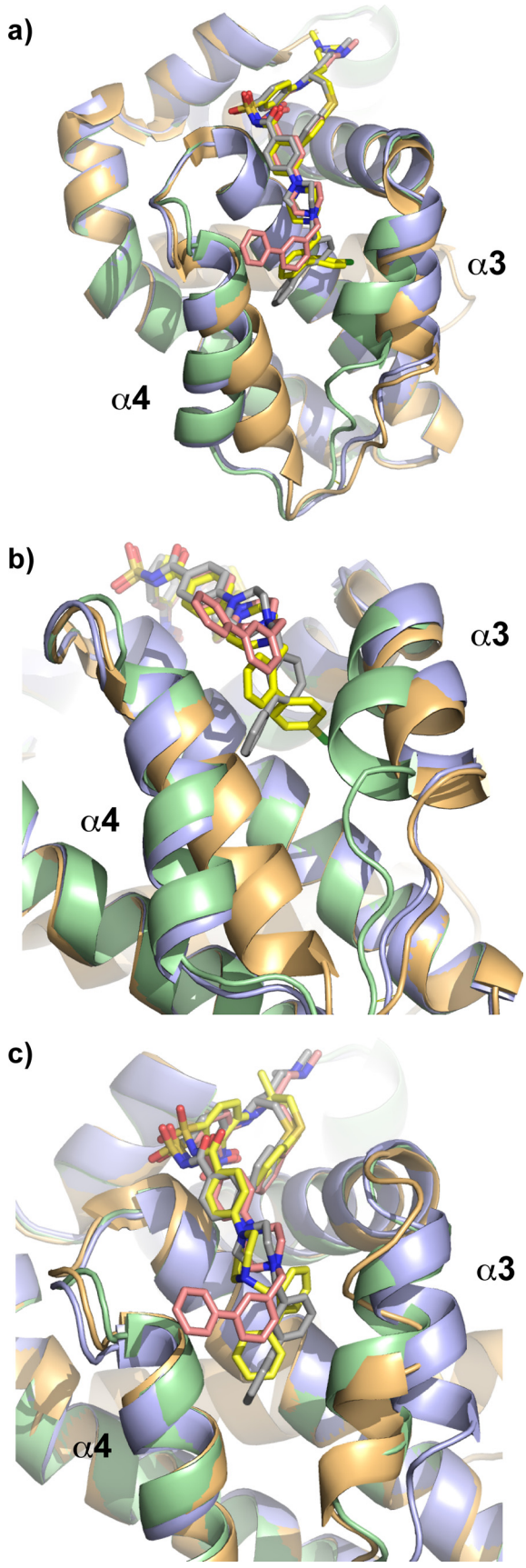

FIGURE 4. **Structure of the W1191542·Bcl-x_L complex.** *a*, overlay of structures of Bcl-x_L in complex with ABT-737 (Bcl-x_L, *orange*; ABT-737, *yellow*), W1191542 molecule A (Bcl-x_L, *green*; W1191542/A, *pink*), or W1191542 molecule B (Bcl-x_L, *blue*; W1191542/B, *gray*). Note the significant differences in the orientation of the α3 and α4 helices. *b*, close-up view of each compound in the region of the h2 pocket. The biphenyl of W1191542 molecule A projects out of the binding groove located between the α3 and α4 helices, whereas in W1191542 molecule B and ABT-737 it projects into the groove, although their orientations are different. *c*, overlay of the structures of Bcl-x_L in complex with Compound 43b (Bcl-x_L, *orange*; Compound 43b, *yellow*) (23), W1191542 molecule A (Bcl-x_L, *green*; W1191542/A, *pink*), or W1191542 molecule B (Bcl-x_L, *blue*; W1191542/B, *gray*). The space occupied by the biphenyl of Compound 43b overlays with that used by the biphenyl moiety in W1191542 molecule B.

ined for its ability to inhibit long term (6 days) clonogenic survival of *mcl-1*$^{-/-}$ MEFs. Again, although clonal suppression was observed with *mcl-1*$^{-/-}$ MEFs (but not *bcl-x*$^{-/-}$ MEFs), it was significantly weaker than ABT-737 (Fig. 3*c*). Hence, the killing potency of MEFs by small molecules appears to be significantly affected by the range of pro-survival proteins they target.

Finally, we examined W1191542 in a direct binding assay using a Biacore S51 instrument that enables the kinetics of small organic compounds binding to their targets to be determined. This approach eliminates some of the limitations of solution competition studies and expands the dynamic range of the assay. Interestingly, this assay provided a similar result to the competition assay, indicating that ABT-737 bound Bcl-x_L ~2-fold tighter than W1191542 (Fig. 3*d* and supplemental Fig. 2). However, the kinetics of the interactions are somewhat different; W1191542 binds Bcl-x_L almost three times faster than ABT-737, but ABT-737 has a greater than 5-fold slower off-rate. The shortened half-life of the W1191542·Bcl-x_L complex, 190 s *versus* 1000 s for the ABT-737 complex, seems a better indicator of its reduced potency than does its K_D.

Structure of W1191542 Complexed to Bcl-x_L—The binding kinetics of W1191542 and ABT-737 suggest that these compounds engage Bcl-x_L differently despite the similarity in their chemical structures (Fig. 2*a*). We were also interested in how W1191542 would bind Bcl-x_L after our modification to ABT-737; that is, whether the biphenyl moiety would now project directly down into the h2 pocket rather than toward the α3 helix. To help address both of these issues, we determined the crystal structure of W1191542 with Bcl-x_L at 2.0 Å resolution using a loop deleted form of Bcl-x_L (41, 47, 48). This variant forms a domain swapped dimer in which the α1 helix of each Bcl-x_L molecule crosses into its neighbor. This domain exchange is distant from, and has no apparent effect on the ligand binding groove (47, 48). The advantage of using this form of Bcl-x_L is that it allows crystals of Bcl-x_L complexes to grow reproducibly within days instead of months, as previously reported (7, 53).

Two W1191542·Bcl-x_L complexes are present in the asymmetric unit, each providing a different view of the interaction between the compound and its target. The major difference is in the biphenyl moiety (Fig. 4); in molecule B the biphenyl penetrates the h2 binding pocket, whereas in molecule A it is rotated around the methyl-biphenyl-piperazine C-N bond ~45° relative to molecule B and projects out of the groove. There is also a discernable difference in the orientation of the α3 helix in molecule B resulting in a wider binding groove. The different crystal environments of molecules A and B are manifest as weak intermolecular contacts involv-

ing the ligand bound to molecule B. In molecule B helix α3 also participates in intermolecular crystal contacts. The two views provided by this structure may have captured the binding groove in transition from the closed to opened state upon ligand binding.

When compared with the ABT-737·Bcl-x_L structure, it is apparent that W1191542 binds similarly with the exception of the chlorobiphenyl moiety on ABT-737, which penetrates the h2 pocket differently from the biphenyl of both molecules in this new structure (Fig. 4, *a* and *b*). There are also significant differences in the orientation of the α3 and α4 helices; the α4 helix (*orange*) in the ABT-737 complex is different in both molecules of the W1191542 complex, whereas the α3 helix adopts a conformation similar to that seen in the molecule where the biphenyl group of W1191542 is buried (*blue*).

Structure of Wild-type Bim and BimL12F Complexed with Bclx_L—The structures of W1191542 and ABT-737 in complex with Bcl-x_L revealed two distinct binding modes, especially in the region of the h2 pocket within the Bcl-x_L hydrophobic groove. We, therefore, examined how a peptide ligand with an aromatic moiety at h2 would engage Bcl-x_L as this could provide further insights into the structural plasticity of Bcl-2 family proteins.

By again using the loop-deleted form of Bcl-x_L (47, 48), we were also able to crystallize and determine structures of both wild-type Bim and the BimL12F mutant in complex with Bcl-x_L (Table 1). These two closely related Bim peptides crystallized in different conditions, suggesting differences in the structures, unlike with Mcl-1, where closely related Bim peptides (wild-type and L12Y) crystallized in very similar conditions and yielded similar structures. The wild-type complex is noticeably different from the previously published structure of the homologous murine complex (7) only at the C-terminal end of the peptide where the murine Bim BH3 extends in helical conformation for two full turns beyond the binding groove on Bcl-x_L (although this feature is an artifact of the crystals of the murine complex and is not observed here). Crystals of the BimL12F·Bcl-x_L complex are twinned and have two molecules in the asymmetric unit; chains A and B describe one peptide-protein complex (AB), and chains C and D describe the other (CD). Helix α3 is poorly resolved in both molecules, although it is somewhat better in the complex CD, which we describe here. Although the overall structure is similar to the wild-type Bim·Bcl-x_L complex (Fig. 5*a*), substantial differences are apparent in helix α3. The side chain of the substituted phenylalanine residue in the h2 position of the peptide penetrates into its binding pocket in a manner very similar to that observed for the chlorobiphenyl group of ABT-737 (Fig. 5*b*) and unlike the biphenyl moiety of W1191542 (Fig. 5*c*).

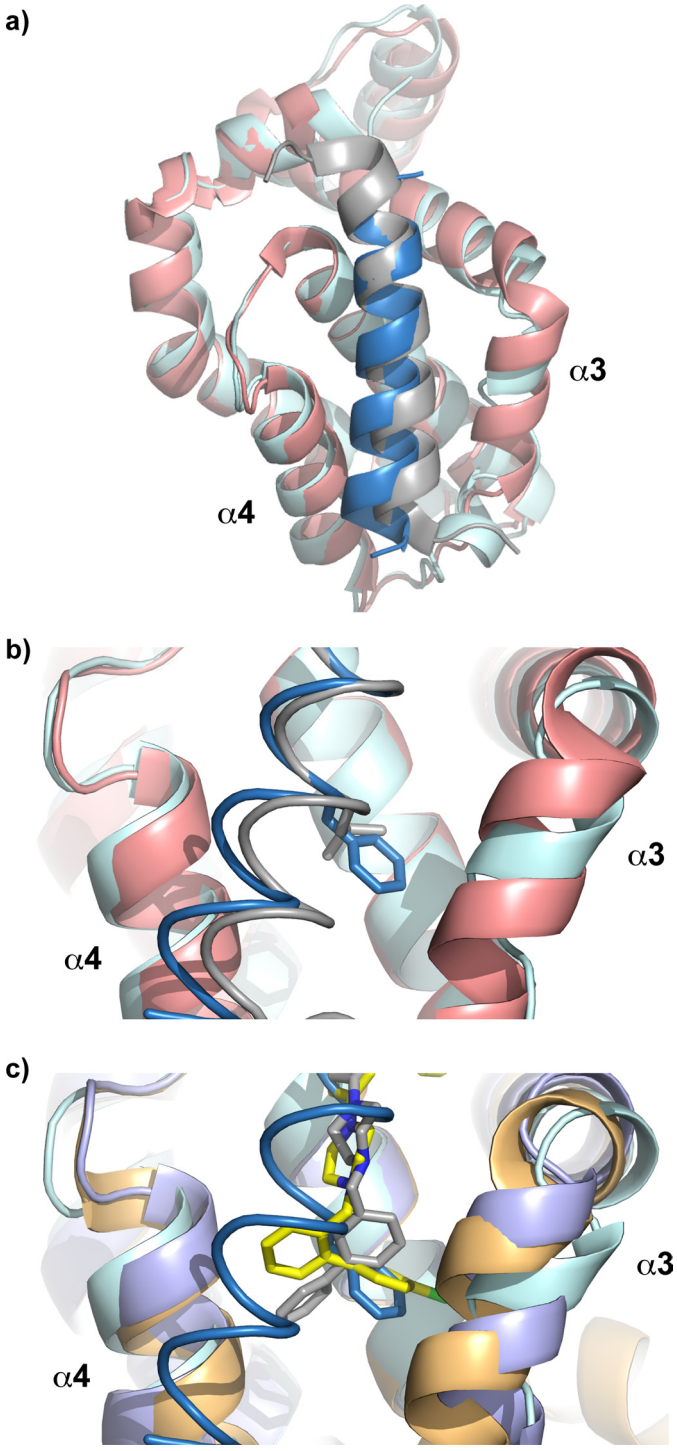

FIGURE 5. **Structure of the BimL12F·Bcl-x_L complex.** *a*, overlay of structures of Bcl-x_L in complex with wild-type Bim BH3 (Bcl-x_L, *pink*; Bim BH3, *gray*) or BimL12F (Bcl-x_L, *cyan*; BimL12F, *dark blue*). *b*, close-up view in the region of the h2-binding pocket showing the relative orientation of the wild-type leucine residue in Bim BH3 (*gray*) or the phenylalanine residue at the same position in the mutated peptide (*dark blue*). *c*, overlay of the structures of Bcl-x_L in complex with BimL12F (Bcl-x_L, *cyan*; BimL12F, *dark blue*), ABT-737 (Bcl-x_L, *orange*; ABT-737, *yellow*), or W1191542 molecule B (Bcl-x_L, *light blue*; W1191542/A, *gray*). The phenylalanine side chain projects into the h2 binding pocket similarly to the chlorobiphenyl moiety of ABT-737.

DISCUSSION

A Novel Bcl-x_L-selective Antagonist—The anti-tumor activity of ABT-737/ABT-263 in cell culture systems in *in vivo* models of cancer and, more recently in human patients, provides incentive to develop further anti-cancer therapeutics of the BH3-mimetic class. An obvious starting point for extending the range of tumors that could be treated with such molecules would be through varying the spectrum of pro-survival proteins they target. An Mcl-1-specific compound is likely to prove useful for cancers such as multiple myeloma, which are dependent on Mcl-1 for their survival (54, 55).

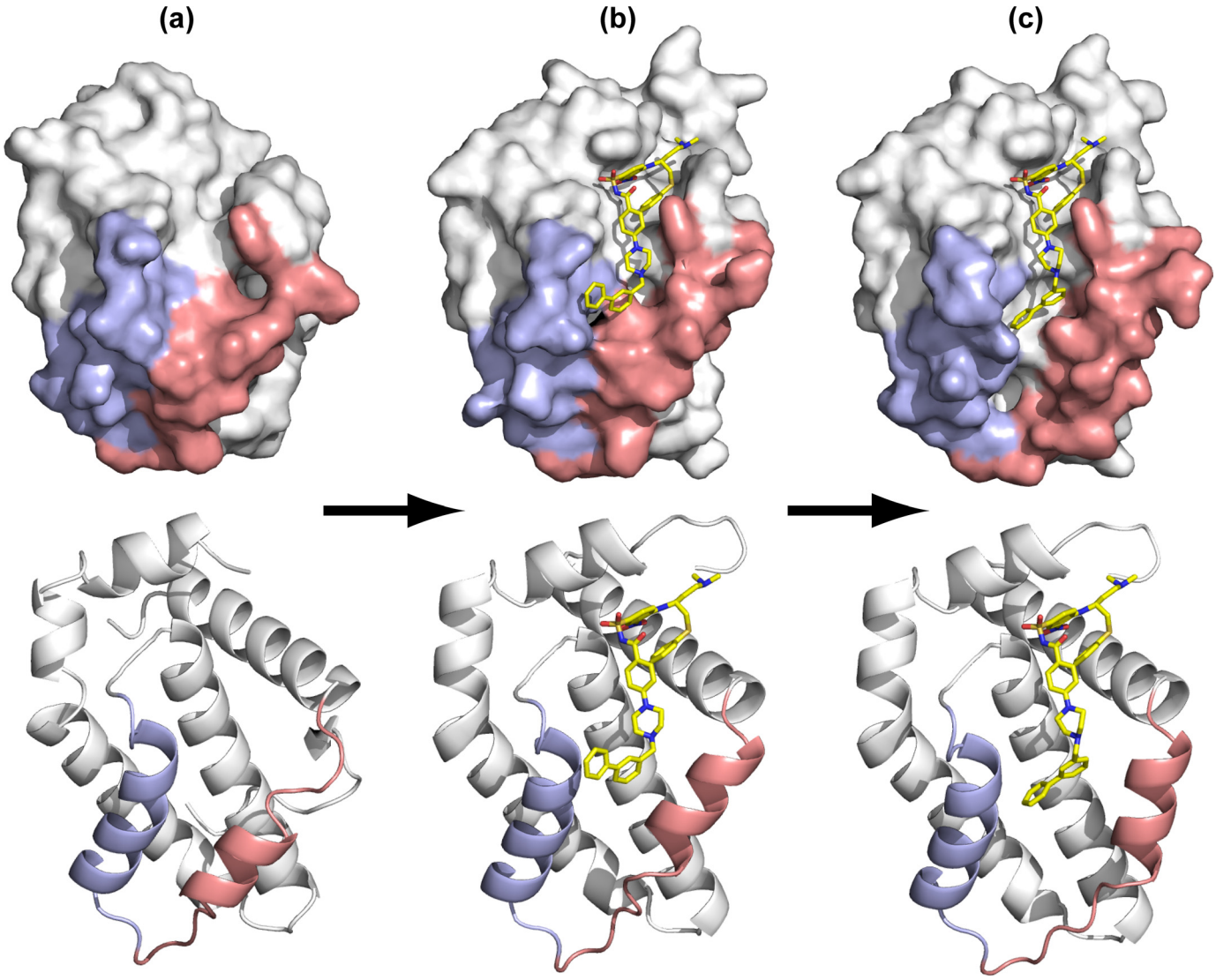

FIGURE 6. **Proposed structural transitions in the binding of W1151952 to Bcl-x_L.** *a*, the lower half of the binding groove (α3 helix, *pink*; α4 helix, *blue*) is occluded in unliganded Bcl-x_L (PDB 1MAZ). *b*, upon engaging W1191542, there is a partial opening of the groove to accommodate the conformer observed in molecule A. *c*, when the biphenyl moiety penetrates the h2 pocket, as in molecule B, the groove is further widened.

Guided by the structures of peptide complexes with Bcl-x_L and Mcl-1 and of ABT-737 with Bcl-x_L, we designed compound W1191542 to acquire binding affinity for Mcl-1. W1191542 shows no significant affinity for Mcl-1 but instead is selective for Bcl-x_L over other pro-survival proteins. Another analogue of ABT-737 (A-385358) with a similar binding profile has been reported previously and shown to be significantly less potent than ABT-737 in both *in vitro* and *in vivo* assays (56). Although this compound was selective for Bcl-x_L over Bcl-2, it also bound to Bcl-x_L weaker than ABT-737, which may account for its reduced activity. However, W1191542 is several orders of magnitude less active than ABT-737 in cell-based assays despite binding Bcl-x_L with only slightly lower affinity (2-fold). Reasons for this apparent discrepancy could include compound solubility and/or cell permeability, different binding kinetics of the compounds to Bcl-x_L, or factors relating to loss of binding of W1191542 to Bcl-2 even though it has previously been shown that in MEFs only Bcl-x_L and Mcl-1 need to be neutralized for Bak-mediated cell death (33).

Bcl-x_L Plasticity—Structural studies of the murine pro-survival Bcl-2 family member A1 concluded that structural plasticity allowed the protein to bind diverse peptide ligands (10). In that case, however, no significant differences in the backbone trace of A1 in the different BH3 peptide complexes are discernable. In contrast, the structures we describe here for Bcl-x_L display large differences in the folding and location of the chain segment connecting helices α2 and α4 and in the position of helix α4. Previous studies have shown that the Bcl-x_L α2-α3 connection is folded differently in the complexes with Bak BH3 (9) and Beclin BH3 (48, 57) compared with the Bim BH3 complex. The structures of the BH3 binding grooves of Bcl-x_L reported here in complex with Bim BH3 L12F and in molecule B of the W1191542 complex are both novel. The structure of the BH3 binding groove of molecule A of the W1191542 complex is similar to the Bcl-x_L complex with Compound 43b (PDB 2O2N) (23).

Especially interesting are the two different views of the W1191542·Bcl-x_L complex in our crystal structure. When com-

bined with the structure of unliganded Bcl-x_L (58), one can speculate about the series of events that lead to the final complex (Fig. 6). For example, if W1191542 from molecule A is overlaid with the unliganded Bcl-x_L, the portion of the molecule from the acyl sulfonamide to the thiophenyl moiety can engage the top half of the groove with minimal overlap. The biphenyl group in this complex projects out of the groove which is more closed in the region of the h2 pocket, notably by Leu-108. In molecule B of the W119542 complex, the groove is widened by the displacement of α3 and the accommodation of the biphenyl moiety in the h2 pocket. In both W119542 complex structures, α4 is unperturbed from its conformation in unliganded Bcl-x_L. However, when ABT-737 binds, α4 is observed to lie closer to α3 than in the W119542 complex structures (see Fig. 4). Hence, molecules similar to ABT-737 may initially engage Bcl-x_L in the h4 pocket, which is relatively "open" in the unliganded structure, and then progressively bind along the groove toward the h1 pocket with coordinated rearrangements in the α3 and α4 helices that open up the groove. It may be that BH3 peptides also bind Bcl-x_L in this way. Notably the speculative structural transition presented in Fig. 6 encompasses the full range of structures observed to date from closed (PDB 1MAZ), partially open, and open (PDB 3INQ).

There is not yet any evidence that the softness in the structure of Bcl-x_L helix α3 is also a property of the Mcl-1 structure. There the BH3 binding groove is apparently more open in the unliganded state (5, 59). Furthermore, there is a striking difference in the accommodation of the Bim BH3 variants L12Y into Mcl-1 and L12F into Bcl-x_L, the former causing only minor local perturbations in the Mcl-1 structure and the latter partially dissolving the α3 of Bcl-x_L. Recently, Fu *et al.* (60) attempted to model a BimL12F variant into Bcl-x_L. Our results showing the significant structural plasticity in Bcl-x_L upon ligand binding (including with BimL12F) highlight the potential challenges involved in such modeling studies that will equally apply to modeling small molecule ligands.

Design Issues—Compound W1191542 did not acquire the capacity to bind to Mcl-1. Saturation mutagenesis of Leu-12 of Bim BH3 (25) showed a 10-fold or less loss of binding of L12Y to Bcl-2, Bcl-w, and Bcl-x_L but a 60-fold loss of binding to Mcl-1. The structure of that mutant complexed to Mcl-1 and reported here suggests little capacity in Mcl-1 to reshape itself around the mutated residue. Thus, a plausible explanation for the failure of W1191542 to bind to Mcl-1 is that Mcl-1 is less forgiving of structural alterations in the h2 pocket. Abbott Laboratories have reported the structure of a complex of Bcl-x_L with a molecule similar to ABT-737, Compound 43b (PDB 2O2N (23)) (Fig. 2*a*) but with the chlorobiphenyl moiety replaced with a biphenyl, as in W1191542 (although the biphenyl group is in the *ortho* position, not *meta*, as in W1191542). The space occupied by the biphenyl of Compound 43b overlays that utilized by the biphenyl of molecule B in the W1191542 complex (Fig. 4*c*). This is achieved through differences in the conformation of the piperazine ring and the torsion angles in the methylene connector to the biphenyl. Thus, we attribute the retention of binding of W119542 to Bcl-x_L to flexibility of both the protein and the compound. These results highlight significant differences in the structural properties of members of the Bcl-2 pro-survival protein family, differences that are likely to be important in the quest for compounds capable of selectively antagonizing the different family members. In conclusion, we suggest that differential binding of the Bcl-2 family members to particular peptides or compounds might reflect their capacity to adopt a compatible conformation to the ligand and not merely amino acid sequence differences among the family members in the ligand binding groove.

Acknowledgments—Infrastructure support from National Health and Medical Research Council IRIISS Grant 361646 and the Victorian State Government OIS grant is gratefully acknowledged. Crystallization trials were performed at the Bio21 C3 Collaborative Crystallization Centre. Data for the BimL12F BH3 complex with Bcl-x_L were collected on the PX1 beamline at the Australian Synchrotron, Victoria, Australia. We thank Abbott Laboratories for provision of ABT-737, David Huang, Andreas Strasser, Philippe Bouillet, Priscilla Kelly, and Mark van Delft for essential reagents, and Madelin Tan for assistance with crystallization.

REFERENCES

1. Cory, S., Huang, D. C., and Adams, J. M. (2003) *Oncogene* **22,** 8590–8607
2. Youle, R. J., and Strasser, A. (2008) *Nat. Rev. Mol. Cell Biol.* **9,** 47–59
3. Fesik, S. W. (2005) *Nat. Rev. Cancer* **5,** 876–885
4. Chipuk, J. E., and Green, D. R. (2008) *Trends Cell Biol.* **18,** 157–164
5. Czabotar, P. E., Lee, E. F., van Delft, M. F., Day, C. L., Smith, B. J., Huang, D. C., Fairlie, W. D., Hinds, M. G., and Colman, P. M. (2007) *Proc. Natl. Acad. Sci. U.S.A.* **104,** 6217–6222
6. Day, C. L., Smits, C., Fan, F. C., Lee, E. F., Fairlie, W. D., and Hinds, M. G. (2008) *J. Mol. Biol.* **380,** 958–971
7. Liu, X., Dai, S., Zhu, Y., Marrack, P., and Kappler, J. W. (2003) *Immunity* **19,** 341–352
8. Petros, A. M., Nettesheim, D. G., Wang, Y., Olejniczak, E. T., Meadows, R. P., Mack, J., Swift, K., Matayoshi, E. D., Zhang, H., Thompson, C. B., and Fesik, S. W. (2000) *Protein Sci.* **9,** 2528–2534
9. Sattler, M., Liang, H., Nettesheim, D., Meadows, R. P., Harlan, J. E., Eberstadt, M., Yoon, H. S., Shuker, S. B., Chang, B. S., Minn, A. J., Thompson, C. B., and Fesik, S. W. (1997) *Science* **275,** 983–986
10. Smits, C., Czabotar, P. E., Hinds, M. G., and Day, C. L. (2008) *Structure* **16,** 818–829
11. Degterev, A., Lugovskoy, A., Cardone, M., Mulley, B., Wagner, G., Mitchison, T., and Yuan, J. (2001) *Nat. Cell Biol.* **3,** 173–182
12. Enyedy, I. J., Ling, Y., Nacro, K., Tomita, Y., Wu, X., Cao, Y., Guo, R., Li, B., Zhu, X., Huang, Y., Long, Y. Q., Roller, P. P., Yang, D., and Wang, S. (2001) *J. Med. Chem.* **44,** 4313–4324
13. Mohammad, R. M., Goustin, A. S., Aboukameel, A., Chen, B., Banerjee, S., Wang, G., Nikolovska-Coleska, Z., Wang, S., and Al-Katib, A. (2007) *Clin. Cancer Res.* **13,** 2226–2235
14. Nguyen, M., Marcellus, R. C., Roulston, A., Watson, M., Serfass, L., Murthy Madiraju, S. R., Goulet, D., Viallet, J., Bélec, L., Billot, X., Acoca, S., Purisima, E., Wiegmans, A., Cluse, L., Johnstone, R. W., Beauparlant, P., and Shore, G. C. (2007) *Proc. Natl. Acad. Sci. U.S.A.* **104,** 19512–19517
15. Oltersdorf, T., Elmore, S. W., Shoemaker, A. R., Armstrong, R. C., Augeri, D. J., Belli, B. A., Bruncko, M., Deckwerth, T. L., Dinges, J., Hajduk, P. J., Joseph, M. K., Kitada, S., Korsmeyer, S. J., Kunzer, A. R., Letai, A., Li, C., Mitten, M. J., Nettesheim, D. G., Ng, S., Nimmer, P. M., O'Connor, J. M., Oleksijew, A., Petros, A. M., Reed, J. C., Shen, W., Tahir, S. K., Thompson, C. B., Tomaselli, K. J., Wang, B., Wendt, M. D., Zhang, H., Fesik, S. W., and Rosenberg, S. H. (2005) *Nature* **435,** 677–681
16. Tzung, S. P., Kim, K. M., Basañez, G., Giedt, C. D., Simon, J., Zimmerberg, J., Zhang, K. Y., and Hockenbery, D. M. (2001) *Nat. Cell Biol.* **3,** 183–191
17. Yin, H., Lee, G. I., Sedey, K. A., Kutzki, O., Park, H. S., Orner, B. P., Ernst, J. T., Wang, H. G., Sebti, S. M., and Hamilton, A. D. (2005) *J. Am. Chem. Soc.* **127,** 10191–10196

18. Yin, H., Lee, G. I., Sedey, K. A., Rodriguez, J. M., Wang, H. G., Sebti, S. M., and Hamilton, A. D. (2005) *J. Am. Chem. Soc.* **127,** 5463–5468
19. Lessene, G., Czabotar, P. E., and Colman, P. M. (2008) *Nat. Rev. Drug Discov.* **7,** 989–1000
20. Prakesch, M., Denisov, A. Y., Naim, M., Gehring, K., and Arya, P. (2008) *Bioorg. Med. Chem.* **16,** 7443–7449
21. Feng, W. Y., Liu, F. T., Patwari, Y., Agrawal, S. G., Newland, A. C., and Jia, L. (2003) *Br. J. Haematol.* **121,** 332–340
22. van Delft, M. F., Wei, A. H., Mason, K. D., Vandenberg, C. J., Chen, L., Czabotar, P. E., Willis, S. N., Scott, C. L., Day, C. L., Cory, S., Adams, J. M., Roberts, A. W., and Huang, D. C. (2006) *Cancer Cell* **10,** 389–399
23. Bruncko, M., Oost, T. K., Belli, B. A., Ding, H., Joseph, M. K., Kunzer, A., Martineau, D., McClellan, W. J., Mitten, M., Ng, S. C., Nimmer, P. M., Oltersdorf, T., Park, C. M., Petros, A. M., Shoemaker, A. R., Song, X., Wang, X., Wendt, M. D., Zhang, H., Fesik, S. W., Rosenberg, S. H., and Elmore, S. W. (2007) *J. Med. Chem.* **50,** 641–662
24. Vogler, M., Weber, K., Dinsdale, D., Schmitz, I., Schulze-Osthoff, K., Dyer, M. J., and Cohen, G. M. (2009) *Cell Death Differ.* **16,** 1030–1039
25. Lee, E. F., Czabotar, P. E., Smith, B. J., Deshayes, K., Zobel, K., Colman, P. M., and Fairlie, W. D. (2007) *Cell Death Differ.* **14,** 1711–1713
26. Ackler, S., Xiao, Y., Mitten, M. J., Foster, K., Oleksijew, A., Refici, M., Schlessinger, S., Wang, B., Chemburkar, S. R., Bauch, J., Tse, C., Frost, D. J., Fesik, S. W., Rosenberg, S. H., Elmore, S. W., and Shoemaker, A. R. (2008) *Mol. Cancer Ther.* **7,** 3265–3274
27. Shoemaker, A. R., Mitten, M. J., Adickes, J., Ackler, S., Refici, M., Ferguson, D., Oleksijew, A., O'Connor, J. M., Wang, B., Frost, D. J., Bauch, J., Marsh, K., Tahir, S. K., Yang, X., Tse, C., Fesik, S. W., Rosenberg, S. H., and Elmore, S. W. (2008) *Clin. Cancer Res.* **14,** 3268–3277
28. Tse, C., Shoemaker, A. R., Adickes, J., Anderson, M. G., Chen, J., Jin, S., Johnson, E. F., Marsh, K. C., Mitten, M. J., Nimmer, P., Roberts, L., Tahir, S. K., Xiao, Y., Yang, X., Zhang, H., Fesik, S., Rosenberg, S. H., and Elmore, S. W. (2008) *Cancer Res.* **68,** 3421–3428
29. Certo, M., Del Gaizo Moore, V., Nishino, M., Wei, G., Korsmeyer, S., Armstrong, S. A., and Letai, A. (2006) *Cancer Cell* **9,** 351–365
30. Chen, L., Willis, S. N., Wei, A., Smith, B. J., Fletcher, J. I., Hinds, M. G., Colman, P. M., Day, C. L., Adams, J. M., and Huang, D. C. (2005) *Mol. Cell* **17,** 393–403
31. Kuwana, T., Bouchier-Hayes, L., Chipuk, J. E., Bonzon, C., Sullivan, B. A., Green, D. R., and Newmeyer, D. D. (2005) *Mol. Cell* **17,** 525–535
32. Fletcher, J. I., and Huang, D. C. (2008) *Cell Cycle* **7,** 39–44
33. Willis, S. N., Chen, L., Dewson, G., Wei, A., Naik, E., Fletcher, J. I., Adams, J. M., and Huang, D. C. (2005) *Genes Dev.* **19,** 1294–1305
34. Willis, S. N., Fletcher, J. I., Kaufmann, T., van Delft, M. F., Chen, L., Czabotar, P. E., Ierino, H., Lee, E. F., Fairlie, W. D., Bouillet, P., Strasser, A., Kluck, R. M., Adams, J. M., and Huang, D. C. (2007) *Science* **315,** 856–859
35. Chen, S., Dai, Y., Harada, H., Dent, P., and Grant, S. (2007) *Cancer Res.* **67,** 782–791
36. Konopleva, M., Contractor, R., Tsao, T., Samudio, I., Ruvolo, P. P., Kitada, S., Deng, X., Zhai, D., Shi, Y. X., Sneed, T., Verhaegen, M., Soengas, M., Ruvolo, V. R., McQueen, T., Schober, W. D., Watt, J. C., Jiffar, T., Ling, X., Marini, F. C., Harris, D., Dietrich, M., Estrov, Z., McCubrey, J., May, W. S., Reed, J. C., and Andreeff, M. (2006) *Cancer Cell* **10,** 375–388
37. Lee, E. F., Czabotar, P. E., van Delft, M. F., Michalak, E. M., Boyle, M. J., Willis, S. N., Puthalakath, H., Bouillet, P., Colman, P. M., Huang, D. C., and Fairlie, W. D. (2008) *J. Cell Biol.* **180,** 341–355
38. Lin, X., Morgan-Lappe, S., Huang, X., Li, L., Zakula, D. M., Vernetti, L. A., Fesik, S. W., and Shen, Y. (2007) *Oncogene* **26,** 3972–3979
39. Varfolomeev, E., Blankenship, J. W., Wayson, S. M., Fedorova, A. V., Kayagaki, N., Garg, P., Zobel, K., Dynek, J. N., Elliott, L. O., Wallweber, H. J., Flygare, J. A., Fairbrother, W. J., Deshayes, K., Dixit, V. M., and Vucic, D. (2007) *Cell* **131,** 669–681
40. Zobel, K., Wang, L., Varfolomeev, E., Franklin, M. C., Elliott, L. O., Wallweber, H. J., Okawa, D. C., Flygare, J. A., Vucic, D., Fairbrother, W. J., and Deshayes, K. (2006) *ACS Chem. Biol.* **1,** 525–533
41. Kvansakul, M., Yang, H., Fairlie, W. D., Czabotar, P. E., Fischer, S. F., Perugini, M. A., Huang, D. C., and Colman, P. M. (2008) *Cell Death Differ* **15,** 1564–1571
42. McPhillips, T. M., McPhillips, S. E., Chiu, H. J., Cohen, A. E., Deacon, A. M., Ellis, P. J., Garman, E., Gonzalez, A., Sauter, N. K., Phizackerley, R. P., Soltis, S. M., and Kuhn, P. (2002) *J. Synchrotron Radiat.* **9,** 401–406
43. Otwinowski, Z., and Minor, W. (1997) *Methods in. Enzymology* **276,** 307–326
44. McCoy, A. J., Grosse-Kunstleve, R. W., Storoni, L. C., and Read, R. J. (2005) *Acta Crystallogr. D Biol. Crystallogr.* **61,** 458–464
45. Read, R. J. (2001) *Acta Crystallogr. D Biol. Crystallogr.* **57,** 1373–1382
46. Storoni, L. C., McCoy, A. J., and Read, R. J. (2004) *Acta Crystallogr. D Biol. Crystallogr.* **60,** 432–438
47. Lee, E. F., Sadowsky, J. D., Smith, B. J., Czabotar, P. E., Peterson-Kaufman, K. J., Colman, P. M., Gellman, S. H., and Fairlie, W. D. (2009) *Angew. Chem. Int. Ed. Engl.* **48,** 4318–4322
48. Oberstein, A., Jeffrey, P. D., and Shi, Y. (2007) *J. Biol. Chem.* **282,** 13123–13132
49. Emsley, P., and Cowtan, K. (2004) *Acta Crystallogr. D Biol. Crystallogr.* **60,** 2126–2132
50. Murshudov, G. N., Vagin, A. A., and Dodson, E. J. (1997) *Acta Crystallogr. D Biol. Crystallogr.* **53,** 240–255
51. Adams, P. D., Grosse-Kunstleve, R. W., Hung, L. W., Ioerger, T. R., McCoy, A. J., Moriarty, N. W., Read, R. J., Sacchettini, J. C., Sauter, N. K., and Terwilliger, T. C. (2002) *Acta Crystallogr. D Biol. Crystallogr.* **58,** 1948–1954
52. Lee, E. F., Chen, L., Yang, H., Colman, P. M., Huang, D. C., and Fairlie, W. D. (2008) *Cell Death Differ* **15,** 1609–1618
53. Liu, X., Zhu, Y., Dai, S., White, J., Peyerl, F., Kappler, J. W., and Marrack, P. (2006) *J. Exp. Med.* **203,** 2953–2961
54. Wuillème-Toumi, S., Robillard, N., Gomez, P., Moreau, P., Le Gouill, S., Avet-Loiseau, H., Harousseau, J. L., Amiot, M., and Bataille, R. (2005) *Leukemia* **19,** 1248–1252
55. Zhang, B., Gojo, I., and Fenton, R. G. (2002) *Blood* **99,** 1885–1893
56. Shoemaker, A. R., Oleksijew, A., Bauch, J., Belli, B. A., Borre, T., Bruncko, M., Deckwirth, T., Frost, D. J., Jarvis, K., Joseph, M. K., Marsh, K., McClellan, W., Nellans, H., Ng, S., Nimmer, P., O'Connor, J. M., Oltersdorf, T., Qing, W., Shen, W., Stavropoulos, J., Tahir, S. K., Wang, B., Warner, R., Zhang, H., Fesik, S. W., Rosenberg, S. H., and Elmore, S. W. (2006) *Cancer Res.* **66,** 8731–8739
57. Feng, W., Huang, S., Wu, H., and Zhang, M. (2007) *J. Mol. Biol.* **372,** 223–235
58. Muchmore, S. W., Sattler, M., Liang, H., Meadows, R. P., Harlan, J. E., Yoon, H. S., Nettesheim, D., Chang, B. S., Thompson, C. B., Wong, S. L., Ng, S. L., and Fesik, S. W. (1996) *Nature* **381,** 335–341
59. Day, C. L., Chen, L., Richardson, S. J., Harrison, P. J., Huang, D. C., and Hinds, M. G. (2005) *J. Biol. Chem.* **280,** 4738–4744
60. Fu, X., Apgar, J. R., and Keating, A. E. (2007) *J. Mol. Biol.* **371,** 1099–1117